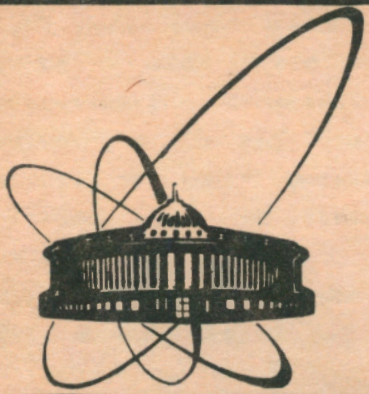

сообщения
объединенного
института
ядерных
исследований
дубна

E17-91-136

U.Wenschuh*, E.Heiner

ON THE THEORY OF ULTRAFAST TRANSIENT OPTICAL PROPERTIES OF LASER EXCITED NOBLE METALS

*University Jena, FRG

1991

1. Introduction

The rapid developments on the fields of pumped dye lasers, light pulse compression and fast detection technique have opened a wide field for the search for phenomena of nonequilibrium dynamics in solid state physics at the beginning of the eightees [1-3].

Because of their outstanding technological applicability semiconductors have attracted most attention [4-8], entire in the opposite to metals.

In semiconductors the relaxation time for excited electron-hole pairs due to scattering with phonons, for instance, has turned out on a ps-timescale [4,5]. For metals a look at the temperature dependence of the specific heats for the electrons and the lattice (see for instance [9]), shows clearly, that, if the electrons can be directly heated on a time scale shorter than the electron-phonon energy relaxation time, a nonequilibrium temperature difference may be possible. This has been the subject of first theoretical investigations several years ago on the basis of an electron gas model [10-12].

Though there had been intense attempts on photoemission studies [13,14] and pump-probe technique [15,16], the observation of transient nonequilibrium processes in metals had been not possible in the first instance. This has been caused by two main difficulties:

(i) Since the high reflectivity of the metals very intense laser pulses ($I \geq 1 GW/cm^2$) are necessary to impart enough energy to the metal electrons.

(ii) The relaxation processes due to the high carrier densities had been turned out much faster than the equivalent in semiconductors, so that new sources had to be developed which should be allow a sufficient time resolution of the process.

In 1984 a subsequent extension of photoemission studies into the femtosecond regime allowed a measurement of electron cooling but was restricted to high temperatures and suffered from space-charge effects [17].

In 1986 femtosecond thermomodulation transmissivity [18] and reflectivity [19] measurements provided the first opportunity to investigate nonequilibrium electron temperatures and their cooling dynamics in metals.
In 1987 Schoenlein et.al. [20] reported about the generation of nonequilibrium electron temperatures in gold by using 65-fs intense laser pulses, which cools to the lattice on a 2-3 ps time scale.
Because the metals exhibit small changes in optical properties, these investigations had only been made possible through the development of new high-repetition-rate femtosecond sources which provide high sensitivity detection with femtosecond time resolution [21-23].
Since that time the field of ultrafast electronic processes in metals has been moved into the field of view of both theoretics [24,25] and experimentalists [26-29] and it should be of much interest in the next time, such as for cheking theories of superconductivity [24,29].

In this work, basing on [25] a theory is developed which describe the cooling process of a transient nonequilibrium electron temperature in a metal via electron-phonon collisions from the point of view of macroscopic quantum statistics by means of a modern version [44,45] of Robertsons time dependent projection technique [46].
The considerations will be restricted to noble metals, since its novel electron band structure allows to treat the electron system in a clear and simple way, as it will be discussed in detail in section 2.
To suppress spatial inhomogenities and therefore heat diffusion effects, the theory will be restricted to layer material ($d \leq 100nm$), too.
The work results in the obtaining of numerical casted time dependent spectra of the reflectivity, monitoring the transient cooling process and giving a direct comparision to recent experimental results [20].

In section 3 the model Hamiltonian is presented and a differential equation system is derived describing the energy loss rates in the thermalized (hydrodynamical) stage of evolution. It is reformulated to a system for the time evolution of the electron and the phonon temperature what is casted out over a coarse grained, i.e. macroscopical time axis.
In section 4 a macroscopic dielectric function (MDF) adapted to the problem is presented describing the optical response of a weak probe pulse testing in time the evolution of the cooling process.
In section 5 numerical calculations for the thermal induced transient alterations of the reflectivity, the optical conductivity and the loss function are carried out for gold with respect to the experiments [20]. A summary and an outlook are given in section 6.

2. Electronic Properties of the Noble Metals and Experimental Setup

2.1. Band Structure of the Noble Metals

Because of its novel electron structure (Cu:KLM$4s^1$, Ag:KLMN$5s^1$, Au:KLMNO$6s^1$) the noble metals have a very advantageous band structure for studying optical properties [30-32]. The Fermi energy lies distant above the flat d-electron bands which form in terms of its energy a localized area of electrons in the density of states, like it is shown in fig.2.1 [33].
It is clearly recognizable that for d-s-interband transitions being investigated chiefly, the basic physics being important for the optical properties is acting distant above the intricate d-electron part of the density of states. It can be considered as a reservoir of electrons for optical interband transistions, the concrete electron structure of it but is out of importance.
Therefore a Fermi shifting of the order of kT do not alter

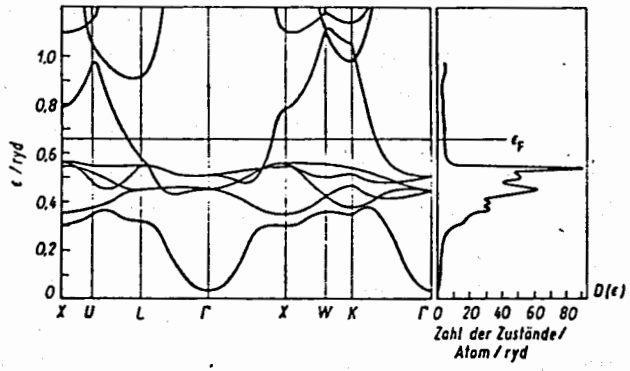

fig.2.1: band structure and density of states of Cu [33]

completely the basic physical situation, what in contrast would be the fact if the Fermi energy would be lying in the d-band area like in transition metals. Consequently, the noble metals enjoy much interest of experimental groups for the investigation of nonequilibrium electron temperatures [15-20,26-29].

2.2 Transient Thermoreflectance Spectroscopy (TTRS)

Modulation spectroscopy utilizes a general principle of experimental physics in which a small perturbation periodically applied to the sample leads to derivative-like features in its optical response. It has been proved as a valuable way of precisely locating critical points in the interband absorption of solids [34,35]. In dependence on the type of the applied perturbation electroreflectance, photoreflectance, thermo- reflectance and piezomodulation spectroscopy are distingueshed.

In thermomodulation measurements a small (1-10K) temperature wave is applied to the sample and the resultant ac component in the reflectivity and/or transmission is measured.

In equilibrium such experiments have been performed for the noble metals in detail by Scouler [36] and Rosei and Lynch [37].

G.L.Eesley [15,16,20] has extended this method to the nonequilibrium by using high repetion rate femtosecond laser sources [21-23]. In this so called TTRS-measurements, see fig.2.2, a first high intensity (outputpower several hundred mW) pump pulse

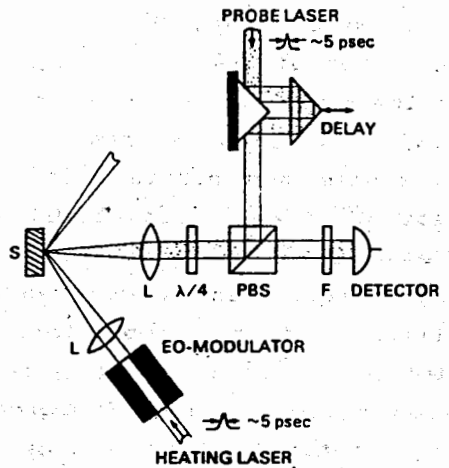

fig.2.2: optical schematic of the TTR-arrangement

brings the electron-phonon system to the nonequilibrium by exciting the electron system to a nonequilibrium quasi temperature lying above the lattice temperature (we disregard here the athermal stage).

Then weak (average power <2mW) continous probe pulses being delayed in time to the pump pulse and acting perpendicular to the sample are proving the changes in reflectivity during the evolution of the excited system toward to the equilibration of both temperatures.

For a comprehensive description of the experimental details I refer to [38].

Note, that the great advantage of the TTRS-measurements in comparison to photoemission experiments [17] is, that only a

small effective increase of the electron temperature arises, what justifies more the approximations for the temperature dependence of the specific heat of the metals and for the heat transport being necessary to perform in theoretical investigations [16,24,25].

3. Bogoljubov's Relaxation Time Hierarchy - Application to Highly Excited Electron Plasma in Metals

An important phenomenon of nonequilibrium processes is the contraction of the number of observables being necessary for the description of the system with passing time.
Due to Bogoljubov [39,40] a succession of contracted descriptions of a system are possible if there exists an accompanying succession of relaxation times such that after each time one has elapsed correlations with lifetimes smaller than this time length are damped out and can be ignored, and increasingly simplified statistical operators can be used for a proper description of the system macrostate. This phenomenon is called *relaxation time hierarchy* and recently has been discussed in detail by Vasconcellos et.al. [41] for the case of highly photoexcited plasma in semiconductors. The main features are in principle the same for highly excited metals. Therefore we want to specialize and present a relaxation time hierarchy for hihgly photoexcited electron plasma in metals:

<u>initial stage:</u> At this point the system can only be described by the statistical operator for the whole system of electrons and ions $\rho(x_1,\ldots,x_N;x'_1,\ldots,x'_N;t)$, given here in coordinate representation or the whole set of reduced statistical operators $\rho_s(x_1,\ldots,x_s;x'_1,\ldots,x'_s;t)$ for one,two,...,s-fold, $s\leq N$, particle complexes. All of them vary rapidly in time for $s\leq 2$, and only the first distribution $\rho_1(x,x',t)$, not involving directly the pair interactions, will vary slowly [40].
But the initial stage cannot be completely specified and the

nonequilibrium processes are determined by a lot of quantities and there is no satisfactory treatment of the problem in this stage.
Furthermore this stage cannot be observed with the time resolution of the existing exciting and detection technique.

Initial Excitation

— 0

INITAL STAGE

No contraction of description

— $\tau_\mu \leq 1$fs

KINETIC STAGE

Description of carriers and phonons

by one-particle statistical operators

— $\tau_1 \leq 10$fs

HYDRODYNAMIC STAGE

Carrier and phonon quasi-temperatur,

quasi-chemical potential

— ↓ Evolution towards equilibrium

<u>first kinetic stage:</u> We need to consider several subsystems, the electron fluid and the ion-lattice.
The dynamics of the latter can be described by the branches of acoustic phonons and it remain the very weak anharmonic [85] and the relatively weak [24] electron-phonon interaction. Hence, practically, from the very outset the phonon system can be described in terms of one-particle statistical operators.
A different situation arises for the electron fluid as a result of the presence of the strong Coulomb interaction. In this case we must look for the collision time τ_μ, given by

$$\tau_\mu \sim \frac{r_o}{v_{av}} . \qquad (3.1)$$

r_o...collision length

v_{av}...average velocity of the particles

With the Fermi velocity $v_F=v_{av}=(\hbar/m^*)(3\pi n)^{1/3}$ and the Thomas-Fermi screening length [42] $\lambda_{TF}=r_o=(\varepsilon\varepsilon_o m^* v_F^2/2ne^2)^{1/2}$ it follows [41]:

$$\tau_\mu \sim \frac{1}{\omega_p} \qquad (3.2)$$

where ω_p is the well known plasma frequency. Here n is the concentration of the carriers, m^* is the carrier effective mass and ε is the static dielectric background constant. For the noble metals $\varepsilon\sim1$, $m^*\sim1$ [43] and then

$$\tau_\mu \sim \frac{1}{\omega_p} \approx 1.8\times10^{-2}/n^{1/2}\ \text{s} . \qquad (3.4)$$

For d-s-band excitations above the Fermi energy the relevant nonequilibrium electron density is equal to that one of the s-band, namely for noble metals $n\sim6\cdot10^{28}m^{-3}$ [44], and it follows, that $\tau_\mu\sim7\cdot10^{-17}$s, i.e. $\tau_\mu \approx 0.1$fs.
Because of the energy mismatch between the photoinjected carriers and the unexcited ones, a number of collisions is necessary to bring the electron system to local equilibrium. Certainly, after a 10fs time scale has elapsed, the metal electron system should be in local equilibrium [16].
This explaining that inspite of the femtosecond time resolution of the laser spectroscopy devices [20-23], the single-particle description of the electron system in metals is well justified because of the high electron densities.

hydrodynamic stage: As discussed above, a very short time being necessary for the internal thermalization of the

electron system because of the strong Coulomb interaction and a further contraction in the description of the macrostate of the carriers subsystem should be possible.
For the case of a homogenous metal electron plasma one may expect that such a description can be made in terms of the quasiequilibrium distribution functions of the carriers, i.e. the number occupation function $f(\varepsilon,T_e(t),\mu_e[T_e(t)],t)$, where ε is the energy of the quasi particle state, $T_e(t)$ is the nonequilibrium quasi-temperatur, $kT_e(t)=\beta_e^{-1}(t)$, and $\mu_e[T_e(t)]$ is the quasi chemical potential.
Since the carriers are fermions, we have

$$f(\varepsilon,t) = \{1+\exp(\beta_e(t)[\varepsilon-\mu_e(t)])\}^{-1} \qquad (4.5)$$

with $\beta_e(t)$ and $\mu_e(t)$ connected to the average density

$$n(t) = \frac{1}{V}\cdot\int_0^x d\varepsilon\cdot g(\varepsilon)\cdot f(\varepsilon,t) \qquad (4.6)$$

where $g(\varepsilon)$ is the density of states function.
From this point the electron-phonon interaction is the dominant process driving the excited system towards to equilibrium.

4. Hydrodynamic Stage in Laser Excited Noble Metals

4.1.Theoretical Model

We use the model Hamiltonian has been proposed in [25] for a highly excited noble metal:

$$\mathcal{H} = \sum_k \sum_{\nu=s,d} \varepsilon(k,\nu) a^+_{k\nu} a_{k\nu} + f(t) \sum_k (\phi_k e^{-i\omega t} a^+_{ks} a_{kd} + \text{h.c.}) +$$

$$+ \sum_{q\mu} \sum_k g_\mu(q) a^+_{ks} a_{k+qs} (b^+_{q\mu} + b_{-q\mu}) + \sum_{q\mu} \omega_{q\mu} (b^+_{q\mu} b_{q\mu} + 1/2)$$

$$= H_e + H_{e\text{-field}} + H_{e\text{-L}} + H_L \qquad (4.1)$$

Here, $\varepsilon(k,\nu=s,d)$ are the single-particle band energies of nonhybridized model bands (Chapter 20 in [62]), $\phi_{\underline{k}}=(e\underline{A}/mc)\langle \underline{k},s|\hat{p}|\underline{k},d\rangle$ is the transfer matrix element, $\underline{A}$ is the vector potential and f(t) is the envelope function of the laser pulse, respectively.

The interaction term $H_{e\text{-field}}$ is treated in the dipole and rotating wave approximation. The electron-phonon coupling parameter $g_\mu(q)$ of the Fröhlich-like electron-phonon interaction term $H_{e\text{-L}}$ is roughly estimated by $|g_\mu(q)|^2=\alpha\omega_D E_F$, where ω_D is the Debye frequency, E_F is the Fermi energy and α is of an order of unity [24,25]. For a direct comparison with experimental results it is desirable to introduce the intensity of the laser pulse into the interaction term $H_{e\text{-field}}$ [46].

We start from the explicit expression for the laser intensity which is given by the time derivative of the Poynting-vector as

$$I = \tfrac{1}{2}\,\varepsilon_o c|\mathcal{E}|^2 \qquad (4.2)$$

where $\mathcal{E}$ is the vector of the electric field. It is expressed in terms of the vector potential by the well-known Maxwell equations

$$\mathcal{E}(t) = -c^{-1}\partial_t \mathcal{A}(t) \qquad (4.3)$$

The time dependence of the vector potential is given as

$$\mathcal{A}(t) = A_k(t)e^{-i\omega t} + \text{h.c.}(k = 1,2,3), \qquad (4.4)$$

where $A_k(t)$ is the envelope function of the amplitude. For the absolute value of the electric field vector $|\mathcal{E}|$ one obtains

$$|\mathcal{E}(t)| = \frac{\omega}{c}\,|\mathcal{A}(t)| + \frac{1}{c}\,\partial_t|\mathcal{A}(t)| \qquad (4.5)$$

in (4.2). The second term in (4.5) is neglected because of the slow alteration of the amplitude envelope function in

comparison with the fast oscillating carrier frequency. For pulse durations of $\tau\approx$100fs this is a well satisfied approximation. For the transfer amplitudes one obtains

$$\phi_{\underline{k}} = \left[\frac{2I}{\varepsilon_o c}\right]^{1/2}\frac{e}{m\omega}\,\langle \underline{k},s|\hat{p}|\underline{k},d\rangle\ . \qquad (4.6)$$

The square of the transfer amplitude can be rewritten in terms of the longitudinal oscillator strength [47,48]

$$f_{\underline{k}sd} = \frac{2|\hat{p}_{\underline{k}sd}|^2}{m(\varepsilon_{\underline{k}s}-\varepsilon_{\underline{k}d})} \qquad (4.7)$$

to [46]:

$$|\phi|^2 = \frac{\hbar e^2 I}{m\omega\varepsilon_o c}\,f_{\underline{k}sd}\ . \qquad (4.8)$$

The complex density of states [30-32], obtained in these papers from first-principle band structure calculations for real nobel metals, corresponding with the considerations in sec.2.1 is replaced by a simple so called Friedel model [25,49] for the density of states, as suggested in [45] and sketched in fig.4.1.

For the broad s-band states free electron behaviour and a spherical Fermi surface is assumed, whereas for the d-band states localized behaviour is postulated. The sum over the

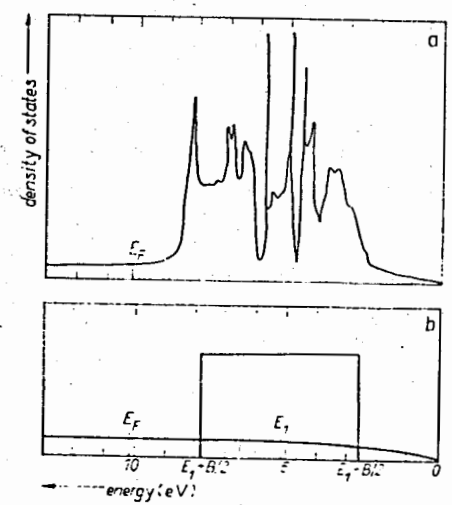

fig.4.1: Friedel-model for the density of states

spin projection of the electrons is included in the band indizes (5.1).

4.2. Evolution Equations

To obtain evolution equations for a macroscopic description the following observation level is picked up by a set of devices for macroscopic measurements [50]:

$$\hat{\Omega} = \{ \hat{1}, \hat{H}_e, \hat{H}_L, \hat{N}_e \} = \{\hat{O}_i\} \tag{4.9}$$

It corresponds to a set of macroscopic Lagrange multipliers

$$\Lambda = \{\lambda_0, \beta_e, \beta_L, -\mu\beta_e\} = \{\lambda_i\} , \tag{4.10}$$

where $\beta_e=(kT_e)^{-1}$ and $\beta_L=(kT_L)^{-1}$. The corresponding reduced statistical operator σ_0 which allows to calculate the expectation values of the relevant observables correctly, has the analytic form

$$\sigma_0 = \exp \{ \lambda_0 1 - \beta_e(\hat{H}_e - \mu\hat{N}_e) - \beta_L\hat{H}_L \} \tag{4.11}$$

It is a solution of the operator integro-differential equation

$$(i\partial_t - \mathbb{P}(t)\mathbb{L}(t))\sigma_0(t) =$$

$$= -i\mathbb{P}(t)\mathbb{L}(t) \int_{-\infty}^{t} ds\ \mathbb{T} \exp\{-i\int_{s}^{t} dt'\mathbb{Q}(s')\mathbb{L}(s')\mathbb{Q}(s')\}\ \mathbb{Q}(s)\mathbb{L}(s)\sigma_0(s) \tag{4.12}$$

where, in superoperator formalism, $\mathbb{L}$ is the corresponding Liouvillean to H and $\mathbb{P}$ ($\mathbb{Q}=1-\mathbb{P}$) is the time dependent projector.

$$\mathbb{P} = \sum_{i,j} |\overset{\sim\sigma_0}{O_i})K_{ij}(O_j| \tag{4.13}$$

with the Kubo transform [51]

$$\overset{\sim\sigma_0}{O_i} = \int_0^1 dx\ \sigma_0^x O_i \sigma_0^{1-x} \tag{4.14}$$

and the matrix

$$(K^{-1})_{l,m} = \mathrm{Tr}\ \overset{\sim\sigma_0}{O_l} O_m \tag{4.15}$$

As already discussed in sec.2 we want to describe the evolution in the hydrodynamic regime. Therefore we substitute the microscopic time axis by a macroscopic one, delayed in time intervals of $\Delta t \approx 10$fs what is the estimated time being the necessary time for establishing the local equilibrium of the electron system.
Now we can perform the short memory approximation (SMA) [25] ($s' \to t, \mathbb{Q}\mathbb{L}\mathbb{Q}=\mathbb{L}_0+\mathbb{Q}\mathbb{L}_1\mathbb{Q} \approx \mathbb{L}_0$) and (5.12) reduces to a much simpler form:

$$(i\partial_t - \mathbb{P}(t)\mathbb{L}(t))\sigma_0(t) =$$

$$-i\mathbb{P}(t)\mathbb{L}(t) \int_{-\infty}^{0} ds\ e^{is(\mathbb{L}_e(t)+\mathbb{L}_L(t))}\ \mathbb{Q}(t)\mathbb{L}(s+t)\sigma_0(t) \tag{4.16}$$

$\mathbb{L}_e, \mathbb{L}_L$ are the Liovillians corresponding to H_e, H_L, respectively. After multiplying (4.16) with the elements of the observation level Ω (4.9) from the left and trace operation, one obtains after some analytical reformulation the equations [25]

$$\partial_t \langle \hat{1} | \sigma_0 \rangle = 0 \tag{4.17}$$

$$\partial_t \langle \hat{N}_e | \sigma_0 \rangle = 0 \tag{4.18}$$

$$\partial_t \langle \hat{H}_e | \sigma_0 \rangle = 4\pi f^2(t)\omega(n_s n_d) \sum_{\vec{k}} |\phi_{\vec{k}}|^2 \delta(\varepsilon(\vec{k},s)-\varepsilon(\vec{k},d)-\omega) *$$

$$*(\langle n_{\vec{k}d} | \sigma_0 \rangle - \langle n_{\vec{k}s} | \sigma_0 \rangle)$$

$$-2\pi \sum_{q\mu} \omega_{q\mu} |g_\mu(q)|^2 n_s \sum_{k} \delta(\varepsilon(k+q,s)-\varepsilon(k,s)-\omega_{q\mu})*$$

$$*(\langle n_{k+q,s}|\sigma_o\rangle\overline{\langle n_{ks}|\sigma_o\rangle}\,\overline{\langle N_{q\mu}|\sigma_o\rangle} - \langle n_{ks}|\sigma_o\rangle\overline{\langle n_{k+q,s}|\sigma_o\rangle}\langle N_{q\mu}|\sigma_o\rangle) \qquad (4.19)$$

$$\partial_t\langle \hat{H}_L|\sigma_o\rangle = 2\pi \sum_{q\mu} \omega_{q\mu} |g_\mu(q)|^2 n_s \sum_{k} \delta(\varepsilon(k+q,s)-\varepsilon(k,s)-\omega_{q\mu})*$$

$$*(\langle n_{k+q,s}|\sigma_o\rangle\overline{\langle n_{ks}|\sigma_o\rangle}\,\overline{\langle N_{q\mu}|\sigma_o\rangle} - \langle n_{ks}|\sigma_o\rangle\overline{\langle n_{k+q,s}|\sigma_o\rangle}\langle N_{q\mu}|\sigma_o\rangle) \qquad (4.20)$$

with $\overline{\langle n_{ks}|\sigma_o\rangle}=1-\langle n_{ks}|\sigma_o\rangle$ and $\overline{\langle N_{q\mu}|\sigma_o\rangle}=1+\langle N_{q\mu}|\sigma_o\rangle$

As discussed in sec.3, the mean square functions can be expressed as Fermi and Bose distribution functions in the hydrodynamic regime. Using

$$\langle n_{ks}|\sigma_o\rangle = \{1+\exp(\beta_e(t)[\varepsilon-\mu_e(t)])\}^{-1}$$

$$= \frac{1}{2}\,(1-\tanh\{\beta_e(t)[\varepsilon-\mu_e(t)]\}) \qquad (4.21)$$

$$\langle N_{q\mu}|\sigma_o\rangle = \{1-\exp(\beta_L(t)[\omega_o])\}^{-1} = \frac{1}{2}\,(\coth\{\beta_L(t)[\omega(q)]\}-1)$$

(4.22)

we get a coupled nonlinear integro-differential equation system which decribes the time evolution of the T_e and the T_L temperatures (θ denote the Debye-temperature) [25]:

$$\partial_t T_i = \frac{3\pi^2}{4}\left(\frac{6n_s}{\pi}\right)^{\frac{1}{3}} \alpha \frac{\omega_D^2}{E_F}\left(\frac{s}{a}\right) \frac{T_e}{\theta}\left(\frac{T_L}{\theta}\right)^2 F_1\left(\frac{T_e}{\theta};\frac{T_L}{\theta}\right) \qquad (4.23)$$

$$F_1 = \frac{\int_{-1}^{1} dx(x+1)\left[\mathrm{cth}\frac{\theta(x+1)}{4T_L} - \mathrm{cth}\frac{\theta(x+1)}{4T_e}\right]\ln\left[\frac{1-\mathrm{th}(\theta(x+1)/4T_e)}{1+\mathrm{th}(\theta(x+1)/4T_e)}\right]}{\int_{-1}^{1} dx(x+1)^4\left[\mathrm{cth}^2\,\frac{\theta(x+1)}{4T_L} - 1\right]} \qquad (4.24)$$

$$\partial_t T_e = \frac{12}{11\pi} f^2(t)\phi^2\omega\left(\frac{E1+\omega}{\mu}\right)^{\frac{1}{2}} \frac{n_s n_d}{T_e}\, j -$$

$$- \frac{3\left(\frac{6n_s}{\pi}\right)^{\frac{1}{3}}}{22(2\pi)^3}\, b\theta^4\alpha\left(\frac{E_F}{\mu}\right)^{\frac{1}{2}}\left(\frac{a}{s}\right)^2 J\left(\frac{T_e}{\theta};\frac{T_L}{\theta}\right) \qquad (4.25)$$

$$j = \int_{-1}^{1} dx\,\left[1+\frac{Bx}{2(E1+\omega)}\right]^{\frac{1}{2}}\left[\mathrm{th}\left(\frac{E1+\omega-\mu+Bx/2}{2T_e}\right) - \mathrm{th}\left(\frac{E1-\mu+Bx/2}{2T_e}\right)\right] \qquad (4.26)$$

$$J = \int_{-1}^{1} dx(x+1)\left[\mathrm{cth}\frac{\theta(x+1)}{4T_L} - \mathrm{cth}\frac{\theta(x+1)}{4T_e}\right]\ln\left[\frac{1-\mathrm{th}(\theta(x+1)/4T_e)}{1+\mathrm{th}(\theta(x+1)/4T_e)}\right] \qquad (4.27)$$

Note that the chemical potential μ_e in (4.21) depends on the

electron temperature, it can be obtained from the particle number conservation

$$n_s\left(\frac{\mu}{E_F}\right)^{3/2}\left(1+\frac{\pi^2}{32}\left(\frac{T_e}{\mu}\right)^2\right)n_d\left[\frac{1}{2}+\frac{T_e}{B}\ln\frac{\cosh\left[(\mu-E1+B/2)/2T_e\right]}{\cosh\left[(\mu-E1-B/2)/2T_e\right]}\right]=n_s+n_d \tag{4.28}$$

5. Macroscopic Dielectric Function (MDF) for Highly Excited Systems

5.1. Arguments for a Description in Linear Response

The optical response in the TTRS-measurements (see sec.2) created by the second weak intensity probe pulse testing delayed in time the transient nonequilibrium stage in the electron-phonon system generated by the high intensity pump pulse.

Certainly, if the probe pulse does not essentially disturb the stage of nonequilibrium evolution, the problem can be considered in a linear response theory. But, usually linear response theories [52] does work in the vicinity of equilibrium. However in our problem there are two well seperated time scales [53]:

(i) the inverse laser frequency of the probe pulse ($\omega^{-1}\approx10^{-16}$s) (fast time scale)

(ii) the relaxation time τ_c due to electron-electron collisions ($\tau_c\approx10^{-14}$s [16]) (smooth time scale)

Following [53] we consider the problem in the fast oscillation frame which oscillates with the laser frequency ω.

Clearly speaken, the slowly varying transient nonequilibrium stage in the electron-phonon system of the noble metal is moving in the fast oscillating frame of the probe puls inverse frequency inside of which the electron-phonon system

can be assumed to be in local equilibrium and the optical response can be evaluated by means of common Greens function technique in linear response.

For a more sophisticated and detailed discussion of the problem of linear response theory far from equilibrium we refer to [53].

5.2. Density-Density-Greens Function in RPA

Starting from the fourier-transformed Maxwell equations and after using the well known Kubo-formula for the linear response of an external perturbed system [52,54], for the longitudinal reciproc dielectric tensor arises:

$$\frac{1}{\varepsilon(q,\omega)} = 1+\frac{e}{4\pi\varepsilon_0 q^2}\sum_{\substack{k\sigma\\ \nu\nu'}}\left|\langle k\nu\sigma|e^{iqr}|k+q,\nu'\sigma\rangle\right|^2\langle\langle c^+_{k\nu\sigma}c_{k+q\nu'\sigma};\rho_{-q}\rangle\rangle^+_\omega \tag{5.1}$$

Here local field corrections have been neglected because of the large wave length of the acting light ($\lambda\approx600$nm) in comparision to the small lattice constant ($a\approx4$nm).

The evaluation of the Fourier transformed density-density-Greens function in (5.1) is carried out by its fourier transformed equation of motion

$$\omega^+\langle\langle c^+_{k\nu\sigma}c_{k+q\nu'\sigma};\rho_{-q}\rangle\rangle^+_\omega = \langle[c^+_{k\nu\sigma}c_{k+q\nu'\sigma},\rho_{-q}]\rangle + \langle\langle[c^+_{k\nu\sigma}c_{k+q\nu'\sigma},\mathcal{H}];\rho_{-q}\rangle\rangle^+_\omega \tag{5.2}$$

with

$$\mathcal{H} = \sum_{k\nu\sigma} \varepsilon_{k\nu} c^{+}_{k\nu\sigma} c_{k\nu\sigma} + \frac{1}{2} \sum_{\substack{kk'qq'\sigma\sigma' \\ \nu\nu'}} v(q)\; c^{+}_{k\nu\sigma} c^{+}_{k'\nu'\sigma'} c_{k'+q\nu'\sigma'} c_{k-q\nu\sigma} \tag{5.3}$$

After a RPA procedure and some algebra for the longitudinal MDF arises the Ehrenreich-Cohen formula [47] which is closely connected to the well known Lindhard formula [55], but here the carrier density is developed into Bloch functions [56] instead of plane waves.

$$\varepsilon(q,\omega) = 1 - \frac{2e^2}{4\pi\varepsilon_0 \mathcal{V} q^2} \sum_{k\nu\nu'} |\langle k\nu | e^{iqr} | k+q\nu' \rangle|^2 \frac{\langle n_{k\nu} \rangle - \langle n_{k+q\nu'} \rangle}{\omega^{+} - (\varepsilon_{k+q\nu'} - \varepsilon_{k\nu})} \tag{5.4}$$

Here the expectation values of the particle numbers are evaluated by the time dependent relevant statistical operator $\sigma_0(t)$, the Ehrenreich-Cohen formula allows us to calculate the time evolution of the MDF over the macroscopic time axis t, as pointed out in sec.3, [60]

$$\varepsilon(q,\omega,\sigma_0[T_e(t)]) \to \varepsilon(q,\omega,t) \quad . \tag{5.5}$$

5.3. Optical MDF

5.3.1. Boundary Transition $q \to 0$

For the purpose being pursued here to describe macroscopic optical properties of the probe-puls light such as reflectivity, loss function and optical conductivity, an optical limit of the MDF is sufficient. Therefore we consider the limit $q \to 0$

$$\varepsilon(\omega) = \lim_{q\to 0} \varepsilon(q,\omega), \tag{5.8}$$

what is not an easy task due to the singularity $1/q^2$. But utilizing a usuful operator relation it follows

$$\frac{1}{q^2} |\langle k\nu | e^{iqr} | k+q\nu' \rangle|^2 \approx \begin{cases} 1 & \nu = \nu' \\ \dfrac{\hbar^2 f^{n_q}_{k\nu\nu'}}{2m(\varepsilon_{k\nu} - \varepsilon_{k\nu'})} & \nu \neq \nu' \end{cases} \tag{5.9}$$

where $f^{n_q}_{k\nu\nu'}$ is the so called longitudinal oscillator strength projected on the unit vector n_q [47,48].

$$f^{n_q}_{k\nu\nu'} = \frac{2|n_q \hat{r}_{k\nu\nu'}|^2}{m(\varepsilon_{k\nu} - \varepsilon_{k\nu'})} \tag{5.10}$$

Now the transition $q \to 0$ can be performed and the MDF is seperated into real and imaginary part.
Note, that the band structure of the noble metal with (5.9) is explicitely involved in the theory.
However, detailed investigations of Uspenski et.al. [57] and Fritzsche [58] show the high expense being necessary to calculate the optical form factors. Following Liang and Beal [59] we circumvent this cumbersome business by setting the oscillator strength constant zero, being a good approximation for calculating optical properties of metals.

5.3.2. Intraband-Part

From (5.8) follows

$$\varepsilon^{intra}(q,\omega) = \frac{2e^2}{4\pi\varepsilon_0 \mathcal{V}} \sum_{k\nu} \frac{\langle n_{ks} \rangle - \langle n_{k+qs} \rangle}{\omega^{+} - (\varepsilon_{k+qs} - \varepsilon_{ks})} \quad . \tag{5.11}$$

After seperating into real and imaginary part it follows

$$\varepsilon^{intra}(\omega) = 1 - \left[\frac{\omega_P}{\omega}\right]^2 . \qquad (5.12)$$

with the plasma frequency in form

$$\omega_P = \left[\frac{n_e e^2}{m_e \varepsilon_o}\right]^{\frac{1}{2}} \qquad (5.13)$$

where n_e is the electron density in the free s-band.

5.3.3. Interband-Part

Seperating the interband part into its real and imaginary part and underlying the simplified model for the density of states, (fig.4.1) and after some lengthy analytical reformulations,which are performed in Appendix A, the following integral expressions result [60]:

$$Re\ \varepsilon^{inter}(\omega) = \frac{(2m)^{\frac{1}{2}}}{\varepsilon_o}\left[\frac{e}{2}\right]^2 \frac{n_s n_d}{(2\pi)^3} f_{Red} * P \int_0^{\infty} dy \int_{-1}^{1} dx \left[G(x,y,+\omega) + G(x,y,-\omega)\right] . \qquad (5.15)$$

$$G(x,y,\pm\omega) = \left[y \pm \omega\right]^{\frac{1}{2}} \frac{th[(\frac{B}{2}x+E_1-\mu)/2T_e] - th[(y\pm\omega-\mu)/2T_e]}{[y-(\frac{B}{2}x+E_1)][y-(\frac{B}{2}x+E_1)\pm\omega]} \qquad (5.16)$$

$$Im\varepsilon^{inter}(\omega) = \left[\frac{m}{2}\right]^{\frac{1}{2}}\left[\frac{e}{4\pi}\right]^2 \frac{n_s n_d}{\varepsilon_o \omega} f_{Red} * * \int_{-1}^{1} dx \left[F(x,+\omega) + F(x,-\omega)\right] \qquad (5.17)$$

$$F(x,\pm\omega) = \left[\frac{B}{2}x+E_1\pm\omega\right]^{\frac{1}{2}} \left\{ th[(\frac{B}{2}x+E_1-\mu\pm\omega)/2T_e] - th[(\frac{B}{2}x+E_1-\mu)/2T_e] \right\} \qquad (5.18)$$

A short analysis shows, that the Kramers-Kronig relations are fulfilled.

5.3.4. Reflectivity, Loss Function and Optical Conductivity

We follow the well known Fresnel formula for the reflectivity

$$R(\omega,t) = \frac{[1-n(\omega,t)]^2 + \varkappa^2(\omega,t)}{[1+n(\omega,t)]^2 + \varkappa^2(\omega,t)} , \qquad (5.19)$$

where $$\sqrt{\varepsilon(\omega,t)} = n(\omega,t) + i\varkappa(\omega,t) \qquad (5.20)$$

with $$\varepsilon(\omega,t) = \varepsilon^{intra} + \varepsilon^{inter} \qquad (5.21)$$

The optical conductivity is defined as

$$\sigma(\omega,t) = \frac{\omega}{4\pi}\varepsilon_2(\omega,t). \qquad (5.22)$$

Because the intraband imaginary part of the MDF can be dropped (see 5.3.2.), the optical conductivity is very

sensitive for excitations near the threshold frequency for interband transitions (see sec.2).
The light field of the laser pulse acting in the layer with the metal electrons lose energy due to inelastic scattering. The loss probability for this process is proportional to the negative imaginary part of the reciprocal MDF [61] and the loss function $l(\omega,t)$ reads

$$l(\omega,t) = [\, - \mathrm{Im}\, \varepsilon^{-1}(\omega,t)\,] = \frac{\varepsilon_2^{\,2}}{\varepsilon_1^{\,2} + \varepsilon_2^{\,2}} \qquad (5.23)$$

6. Numerical Calculations and Discussion

Passing over to a concrete example the expression for $\varepsilon(\omega,t)$ obtained in sec.5 is applied to gold. The parameter set is chosen from several references [9,31,32,44,45] and is gathered in table 1.
The integrals are cast by a Gaussian procedure for each electron temperature which is calculated for a special time t by solving the coupled system of differential equations for T_e and T_L over the macroscopic time axis. At the same time the reflectivity, the loss function and the optical conductivity are computed.
In all the investigations the dimensionless oscillator strength (5.10) is set equal zero because of detailed considerations of Fritzsche [58] have shown that there is a good agreement between calculations of the optical properties of metals with such an approximation and experiment. For each case we have assumed a Gaussian profile of the laser pulse with transfer amplitudes φ_k in form (4.8). The results can be summarized as follows:

Table 1: Parameter set for gold, silver and copper

	Au	Ag	Cu
n_s: number of s electrons per lattice site	1	1	1
n_d: number of d electrons per lattice site	10	10	10
θ : Debye temperature (K) [9]	164	225	343
E_F: Fermi energy with respect to the bottom of the s-band (eV)	10.18[45]	7.49[32]	9.44[31]
E_1: center of the d-band (eV)	5.18[45]	1.81[32]	5.57[31]
B : width of the d-band (eV)	5.28[45]	3.40[32]	3.44[31]
a : lattice constant (nm) [62]	0.4069	0.4079	0.3597
s : averaged sound velocity (nm/ps) [63]	5	5	5
b : number of phonon branches	3	3	3
n : density of conduction electrons ($10^{28}m^{-3}$)[84]	5.9	5.8	8.4
τ : Gaussian pulse width (10^{-14}s)	6.5	6.5	6.5
ω_p: pump frequency (eV)	2.0	3.8	2.0
I : laser intensity (GW/cm^{-2})	60	5	5
T_A: initial-temperature (K)	293	293	293

1.To prove the possibility of utilization of the derived model the real and imaginary parts of the MDF were calculated at T=0.1K and compared with experimental results from [684] which is plotted in fig.6.1.

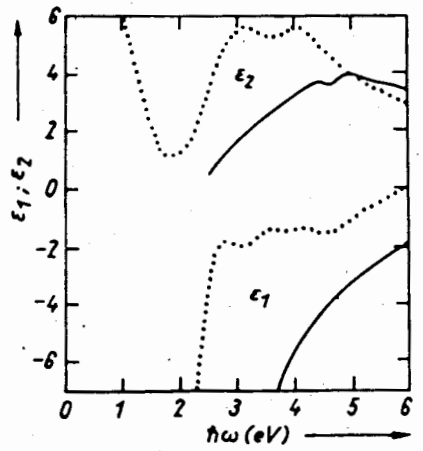

fig.6.1: The MDF $\varepsilon(0,\omega)=[\varepsilon_{\infty}^{-1}(0,\omega)]^{-1}$ for gold at T=0.1K
——— calculated, ····· experimental

Fig.6.1 shows that the basic features of the MDF are described by our model. We note that the model is not able to describe $\varepsilon_2(\omega,t)$ for energies lower than the threshold energy between d- and s-band.

2. The time evolution of the interband part of the MDF for gold after a 100fs pump pulse is casted out. The curves in fig.6.2 show the alterations of the functions caused by the development of the electron temperature from t=0 to that time-point where the function reaches its maximum. After this point the change relaxes in relation with the cooling of the hot electrons by the phonons.
In the presented region of frequencies near the Fermi energy the imaginary part shows a perceived shift to lower frequencies. It is an expression of the Fermi smearing

resulting in a decrease of the minimum frequency for interband transitions. the real part function does not show changes in the presented region.

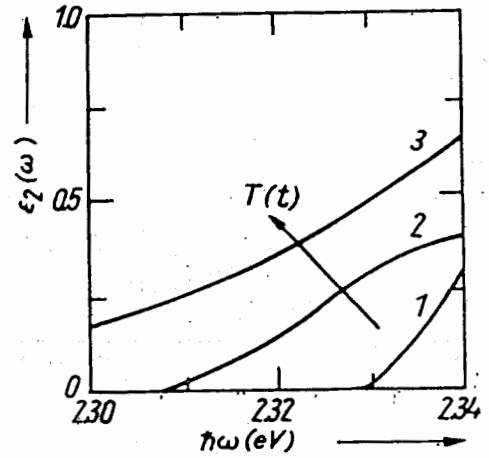

fig.6.2: The evolution of the interband part of the MDF.
(1) t=-200fs, T=50K; (2) t=-40fs, 103K;
(3) t=80fs, 270K.
ω_{pump}=2.5eV, τ=100fs, T_A=50K (the maximum of the pulse is taken at t=0)

3.To have a direct comparison with the experiments in [20] the time evolution of changes in reflectivity for gold is calculated for two probe pulse frequencies represented in figs.6.3a and 6.3b.
The curves show the observed feature of rapid transient increase of reflectivity for time delays of less than 1ps. The relaxation times of about 3 to 4ps are well reproduced. The difference with experiments [20] in fig.6.3b is caused by the fact, that at ω=2.59eV a maximum of the function $\Delta R(\omega)/R(\omega)$ has been observed whereas the calculated function has minima at both points. This references to the problem for

reproducing the function $\Delta R(\omega)/R(\omega)$ with a high degree of exactness.

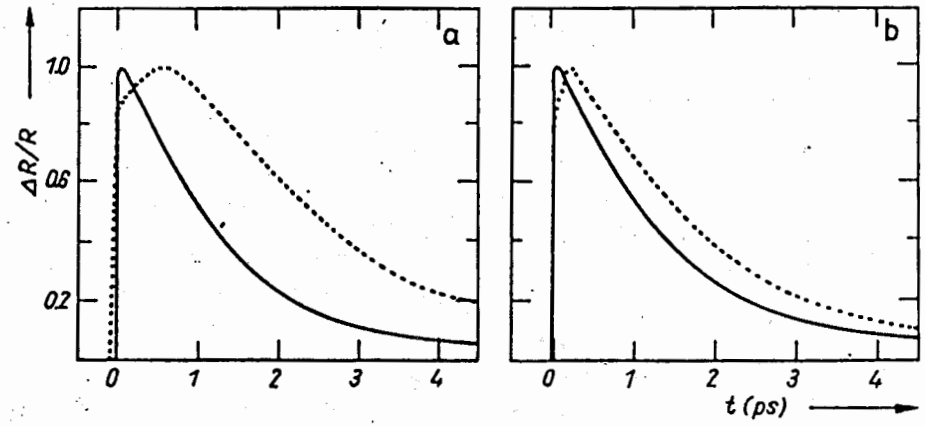

figs.6.3a, 6.3b:
The evolution of the transient reflectivity changes.
a) ω_{probe}=2.59eV and b) 2.69eV. ω_{pump}=2.0eV, τ=65fs, T_A=300K. ——— calculated, ····· experimental

The peak change in reflectivity of the represented curves is $\Delta R/R \approx 10^{-6}$. This is much lower than $\Delta R/R \approx 10^{-2}$ in the reported experiments [20] because in our model with the assumed parameter set the effective increase of the electron temperature is very small. The reasons are the low pump frequency in the course of a high initial temperature and the unknown oscillator strength which is set equal to zero in the model. At lower initial temperatures of about T≈50K the calculated changes of reflectivity are $\Delta R/R \approx 10^{-2}$.

4. The alteration of the reflectivity near the Fermi level is presented for gold in fig.6.4. The time evolution is shown step by step to such a point on the time scale, where $[\Delta R(\omega)/R(\omega)](t)$ has its maximum. The breakdown of the sign of $\Delta R/R$ is obtained at ω=2.44eV which is much larger than the

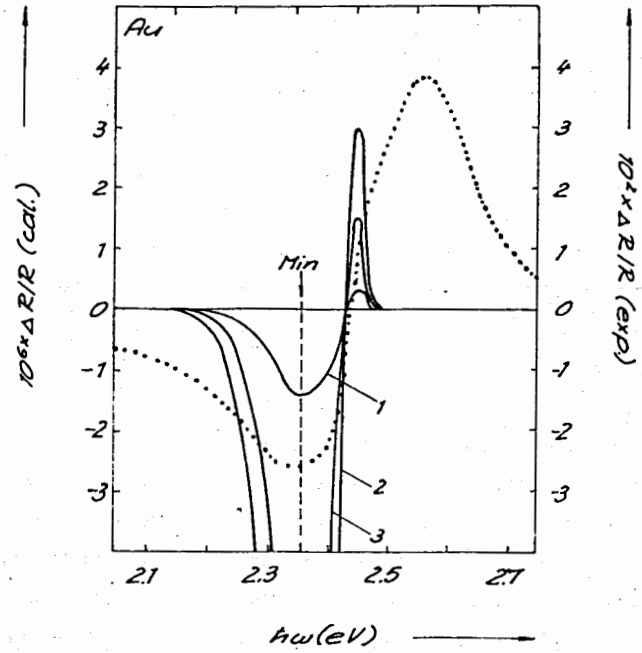

fig.6.4:
Time evolution of $\Delta R(\omega)/R(\omega)$ for gold in the vicinity of the transition threshold energy. (1)t=-40,(2)0,(3)80fs ——— calculated, ····· experimental. (t=0 is the time when the Gaussian pulse shape has its maximum)

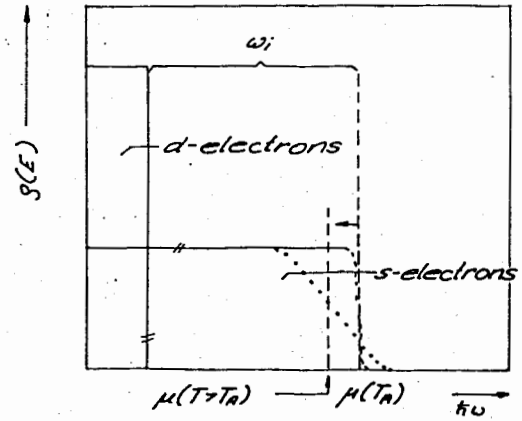

fig.6.5: Time evolution of the electron occupation near the Fermi level

transition threshold of ω=2.38eV. This is simple to understand. If the electron temperature increases due to the pump pulse, the Fermi level smearing takes place in our theory.

However the chemical potential in the model $\mu[T_e(t)]$ is shifted to lower energies if T_e increases in 3D-systems. This results in an enhanced decrease of occupied states below and even above the Fermi level. This effect has its minimum little below the transition threshold energy and leads to a negative increase of the reflectivity changes in this frequency region as plotted in fig.6.5.

For higher frequencies the increase of the occupation results in a positive increase of the change of reflectivity. As is seen in the measured curve of Schoenlein et al. [20] the same features are observed in experiments. Therefore, we can conclude that the most important parameter of the theory is the transition threshold in connection with the temperature dependent chemical potential $\mu(T_e)$ and the use of the simple Friedel model is justified.

However the positive part of $[\Delta R(\omega)/R(\omega)](t)$ from experiments [20] is larger than in our calculation and its maximum lies at a higher frequency. This is caused by the fact that the temperatures have been enriched in the calculations are lower than in experiments, what gives rise to a smaller shift of the chemical potential resulting in a smaller region of effective increase of the occupation. In the same way the magnitude of $\Delta R/R$ is influenced by this temperature discrepancy what is originated in the ignorance of the exact oscillator strength as already mentioned.

Note that the functions in fig.6.4 relax on a time scale of 3 to 4ps. This agrees with the behavior of the plots in figs. 6.3a and 6.3b.

5. Fig.6.6 shows the time evolution of the functions $\Delta\sigma(\omega)/\sigma(\omega)$ and $\Delta l(\omega)/l(\omega)$ in the vicinity of the threshold frequency for interband transitions ω_i for gold, have been calculated in connection with fig.6.4, [66].

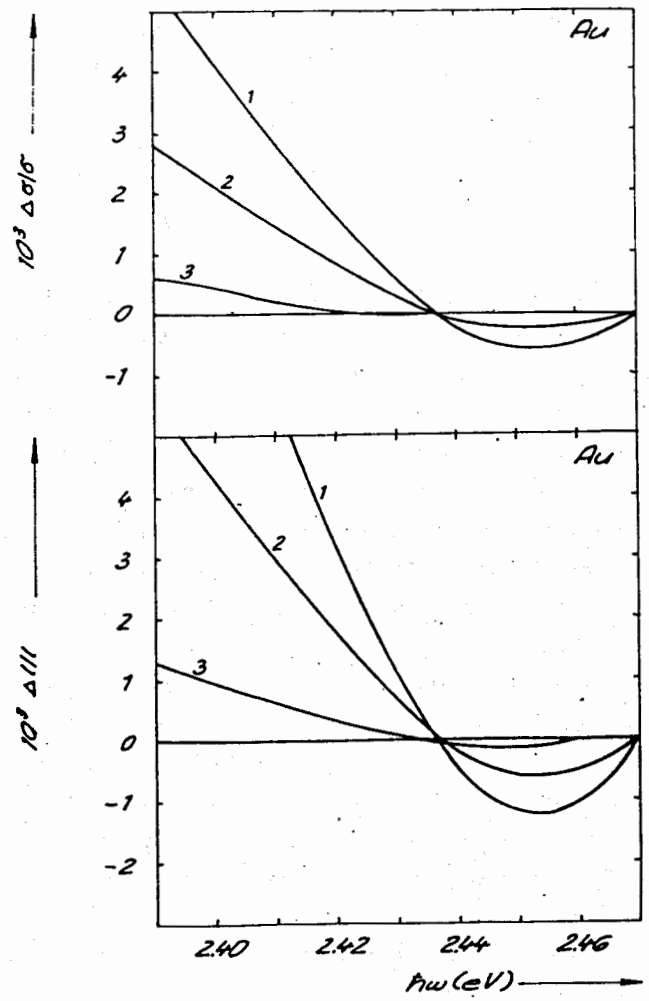

fig.6.6: Time evolution of the $\Delta\sigma(\omega)/\sigma(\omega)$ and $\Delta l(\omega)/l(\omega)$ for gold

As can be seen, the pictures show an increase of the optical conductivity and the loss function below and above of the threshold frequency for interband transitions ω_i with its maximum at ω_i. A change of the signum in $\Delta\sigma$ and Δl is found

at a frequency $\omega_{\pm}>\omega_i$. This is simple to understand with the temperature dependent Fermi level shifting and Fermi smearing whose lead to an effective decrease of occupied states for $\omega<\omega_{\pm}$ and an increase for $\omega_{\pm}>\omega_i$ (see also fig.6.4.).
The positive peaks of $\Delta\sigma/\sigma$ and $\Delta 1/1$ are small because of the small effective increase of occupied states as has been discussed in connection with fig.6.5.
Simply spoken, the optical conductivity has to increase in a frequency region where free electron states exist because energy quants $\hbar\omega$ can absorped and optical currents are able to flow. This again leads to an increase of the energy loss of the incident light which is in our case the probe-pulse-light. For the frequency region where no free electron states exist, an analogous consideration explain the decrease of $\Delta\sigma/\sigma$ and $\Delta 1/1$ as it is shown in fig.6.5. The features are consistent with the calculations of $\Delta R/R$ in figs.6.3a and 6.3b.

6.The functions $[\Delta R(\omega)/R(\omega)](t)$ have been calculated for silver and copper, too.
For silver (fig.6.7) the breakdown of the polarity is placed at ω=4.09eV, the minima of the reflectivity alteration at ω=3.98eV which corresponds to the transition threshold energy for silver. The reason is the same as for gold and has been discussed already above. The alterations of the reflectivity relax in the same way as for gold in figs.7.3a and 7.3b, but on a time scale of about 2ps which is lower than for gold. The reason is the enhanced absolute value of the electron-phonon coupling parameter $|g_{\mu}(q)|^2$.
It should be mentioned that recently a modified pump-probe-technique has been used to study the ultrafast relaxation of electrons probed by surface plasmons in silver films [28]. The curves of $\Delta R/R$ have been observed show the same features like these are discussed here.
For copper (fig.6.8) the breakdown of the polarity is placed at ω=2.26eV and the minima of the reflectivity changes is found at ω=2.15eV.

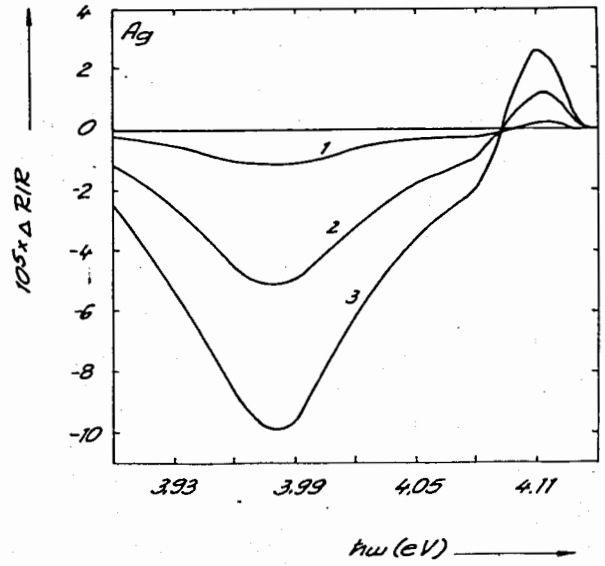

fig.6.7: Time evolution of $\Delta R(\omega)/R(\omega)$ for silver

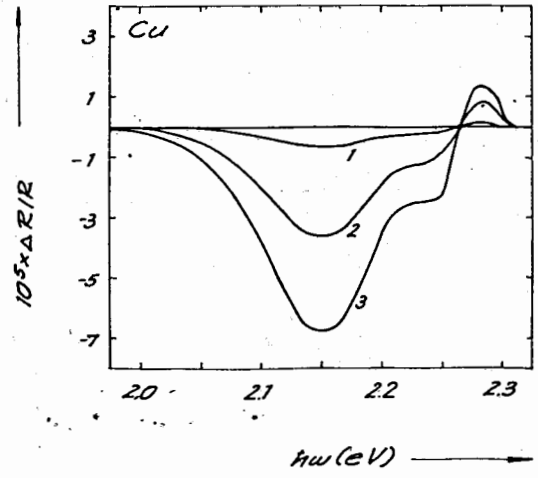

fig.6.8: Time evolution of $\Delta R(\omega)/R(\omega)$ for copper

The significant positive value of $[\Delta R(\omega)/R(\omega)](t)$ at frequencies higher than the transition threshold energy is

well recognizable.
The alterations of the reflectivity are shown in fig.6.9 for three selected frequencies near the transition threshold.
The relaxation time for copper is $\tau \approx 1$ps. It is the shortest of the considered set of noble metals due to the largest electron-phonon coupling parameter.

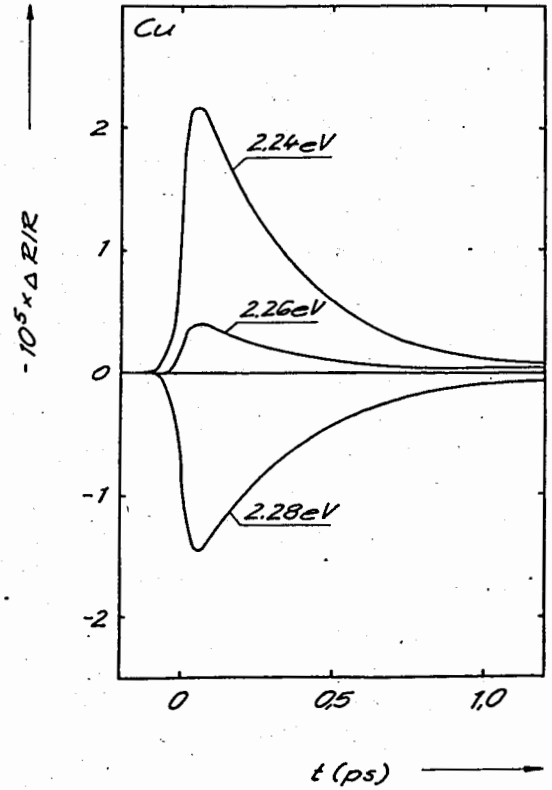

fig.6.9: Breakdown of the sign of $\Delta R/R$ for copper

7. Conclusions

Summarizing, the evolution of laser excited ultrafast transient optical properties in the hydrodynamic stage of thermalized nonequilibrium in noble metal layers can be described with the presented model Hamiltonian, as simple Friedel model for the density of states and a special form of

the macroscopic dielectric function.
The experimental data of the relaxation time for the alteration of the reflectivity function are well reproduced by the numerical calculations.
The smearing of particle occupancy near the Fermi level and the shift of the Fermi level in dependence on the electron temperature lead to a significant ferquency for a polarity reversal of the thermal induced alterations of the reflectivity $\Delta R/R$. It is the most important parameter for comparisions with experiment and it is well reproduced from the theory presented.
A problem remains with the correct reproduction of the magnitude of the reflection alterations which are in the calculations importantly smaller than in the experiments. The explicit introduction of the laser intensity in the light-matter coupling term allows to gain better results and to reduce the problem in the first instance to the oscillator strength has been set equal one in all calculaltions in agreement with detailed band structure investigations [57-59].
However it should be of interest to know the exact value of the oscillator strength. With respect to the simplified Friedel model for the density of states a $\underline{k}$-vector in the middle of the Γ-X axis should be taken. But, even with this specification the numerical expense for performing would be very large.
Another reason for the too small reflectivity alteration in the theory surely lays in the discard of the quasi two-dimensional electron gas structure which is feeled by the laser pulses. Because of the high absorption of the metal ($\approx$10nm penetration depth) the effective electron density and therefore the (surface) plasma frequency are lower than the bulk ones. Surely a consideration of surface plasmon excitations should allow to obtain much more better results [65].
The evaluation of the time evolution of the optical

conductivity and the loss function being consistent with the reflectivity are a resonable completition of the model. There are no experimental curves of these calculated quantities. However this could be carried out for $\Delta\sigma/\sigma$ by using the well adapted differential reflectivity measurement techniques of Beaglehole et.al. [86] in connection with time resolved pump-probe experiments like [15,20] and for $\Delta 1/1$ by using the time resoved absorption spectroscopy or the electron energy loss spectroscopy (EELS) [67].
A exact treatment of the electron-phonon coupling matrix elements have been not necessary for the purpuse pursued here, should allow a checking of the experimental obtained superconductivity constants λ [29] by fitting the experimental curves. From that the T_c-temperatures of the noble metals can be calculated from optical data.

Appendix A - Derivation of the integral forms of the real and the imaginary part of the MDF

After seperation of the interband part of $\varepsilon(\omega)$ into the real and the imaginary part follows

$$\varepsilon^{inter}(\omega) = \sum_{\vec{k}} \frac{\langle n_{\vec{k}s}\rangle - \langle n_{\vec{k}d}\rangle}{\varepsilon_{\vec{k}s} - \varepsilon_{\vec{k}d}} \left\{ P\left[\frac{1}{\omega + (\varepsilon_{\vec{k}s} - \varepsilon_{\vec{k}d})} - \frac{1}{\omega - (\varepsilon_{\vec{k}s} - \varepsilon_{\vec{k}d})} \right] - \right.$$

$$\left. - i\pi \left[\delta(\omega + (\varepsilon_{\vec{k}s} - \varepsilon_{\vec{k}d})) - \delta(\omega - (\varepsilon_{\vec{k}s} - \varepsilon_{\vec{k}d})) \right] \right\} \qquad (A1)$$

From this point real and imaginary part are seperately considered.

a) imaginary part
After transforming the one-particle energies by means of the δ-function follows

$$Im\varepsilon(\omega) = \int_{-\infty}^{\infty} d\omega_1 \int_{-\infty}^{\infty} d\omega_2 \sum_{\vec{k}} \delta(\omega_1 - \varepsilon_{\vec{k}s})\delta(\omega_2 - \varepsilon_{\vec{k}d}) \frac{\langle n_{\vec{k}s}\rangle - \langle n_{\vec{k}d}\rangle}{\varepsilon_{\vec{k}s} - \varepsilon_{\vec{k}d}} *$$

$$* \left[\delta(\omega - (\omega_1 - \omega_2)) - \delta(\omega + (\omega_1 - \omega_2)) \right] \qquad (A2)$$

Since the d-band states have a small dispersion in the $\vec{k}$-space we can destore the so called "nesting" of the δ-functions by assuming the d electrons as $\vec{k}$-independent. Then we can transform the $\vec{k}$-sum into an integration about the density of states.

$$\sum_{\vec{k}} \delta(\omega_1 - \varepsilon_{\vec{k}s})\delta(\omega_2 - \varepsilon_{\vec{k}d}) \approx \frac{1}{N} \sum_{\vec{k}} \delta(\omega_1 - \varepsilon_{\vec{k}s})\delta(\omega_2 - \varepsilon_d) = N\rho(\omega_1)\rho(\omega_2)$$

(A3)

Following the simple Friedel-model of the density of states, presented in sec.4.1, we get

$$\rho(\omega_2) = \begin{cases} h & \text{if } E1 - B/2 \leq \omega \leq E1 + B/2 \\ 0 & \text{otherwise} \end{cases} \qquad h = \frac{1}{B} \qquad (A4)$$

E1 is the middle, B is the width and h is the height of the d-band. The density of states of the free assumed s electrons after introduction of spherical coordinates results in

$$\rho(\omega_1) = \frac{V}{N} \frac{4\pi}{2(2\pi)^3} \frac{(2m)^{\frac{3}{2}}}{\hbar^3} \sqrt{\omega_1}\, \theta(\omega_1)\theta(1.BZ - \omega_1) \qquad (A5)$$

After setting (A3-5) into (A2) and integration about all θ-functions, transforming to a dimensionless integration intervall and transformation of the Fermi function into tanh-form, the formula (5.15,5.16) known from sec.5.3.3 result.

b) real part

Using the assumption in (A3) we get

$$\mathrm{Re}\varepsilon(\omega) = \int_{-\infty}^{\infty} d\omega_1 N n_s \rho(\omega_1) \int_{-\infty}^{\infty} d\omega_2 n_d \rho(\omega_2) \frac{\langle n(\omega_1)\rangle - \langle n(\omega_2)\rangle}{\omega_1 - \omega_2} *$$

$$* \left[P \frac{1}{(\omega + (\omega_1 - \omega_2))} + P \frac{1}{(\omega + (\omega_1 - \omega_2))} \right] \qquad \text{(A6)}$$

After a transformation of the variables $\omega+\omega_1 \to y$ in the first part of (A6) and $\omega-\omega_1 \to y$ in the second part we do the same steps like in a) and get the formula (5.17,5.18) known from sec.5.3.3.

References:

[1] J.Hermann and B.Wilhelmi, Lasers for Ultrashort Light Pulses, Akademie-Verlag, Berlin 1986

[2] S.A.Achmanov, W.A.Wyslouch, A.S.Tschirkin, Optics of Femtosecond Laser Pulses, Nauka, Moscow 1988 (in Russian)

[3] W.Rudolph and B.Wilhelmi, Light Pulse Compression, Harwood Academic Publishers, Chur, London, Paris, N.Y., Melbourne 1989

[4] E.O.Göbel and G.Mahler, in: Festkörperprobleme (Advances in Solid State Physics), Vol.XIX., J.Treusch (ed.), Vieweg, Braunschweig 1979, p.105

[5] D.von der Linde, ibid., p.387

[6] C.Klingshirn and H.Haug, Phys.Rep.70, 315 (1981)

[7] H.Haug and S.Schmitt-Rink, Prog.Quant.Electr.9, 3 (1984)

[8] S.Schmitt-Rink, D.S.Chemla and D.A.B.Miller, Adv.Phys.38, 89 (1989)

[9] C.Kittel, Introduction to Solid State Physics, Geest&Portig, Leipzig 1973, (in German)

[10] M.I.Kaganov, I.M.Lifschitz, and L.V.Tanatarov, Zh.eksper.teor.Fiz.31, 232 (1956); JETP 4, 173 (1957)

[11] S.I.Anisimov, B.L.Kapeloivich, and T.L.Perelman, Zh.eksper.teor.Fiz. 66, 776 (1974); JETP 39, 375 (1974)

[12] S.I.Anisimov, IA.A.Imas, G.S.Romanov, Y.W.Hodyko; Deistvie Islutschenija bolschoi Motschnostji na Metally, Nauka, Moskwa 1970

[13] R.Yen, J.M.Liu, N.Bloembergen, Opt.Commun.35, 277 (1980)

[14] R.Yen, J.M.Liu, N.Bloembergen, T.K.Yee, J.G.Fujimoto and M.M.Salour, Appl.Phys.Lett.40, 185 (1982)

[15] G.L.Eesley, Phys. Rev. Lett. 51, 2140 (1983)

[16] G.L.Eesley, Phys. Rev. B 33, 2144 (1986)

[17] J.G.Fujimoto, J.M.Liu and N.Bloembergen, Phys.Rev.Lett. 53, 1837 (1984)

[18] H.Elsayed-Ali, M.Pessot, T.Norris and G.Mourou, Proceed. of Ultrafast Phemomena V.,Snowmass, Colorado, 1986, in: Springer Series of Chemical Physics, G.R.Fleming and A.E.Siegman (ed.), Vol.46, p.264, Springer, N.Y., 1986

[19] R.W.Schoenlein, W.Z.Lin, J.G.Fujimoto and G.L.Eesley, ibid., p.260

[20] R.W.Schoenlein, W.Z.Lin, J.G.Fujimoto and G.L.Eesley, Phys.Rev.Lett. 58, 1680 (1987)

[21] J.A.Valdmanis, R.L.Fork, and J.P.Gordon, Optics Letters 10, 131 (1985)

[22] W.H.Knox, M.C.Downer, and C.V.Shank, Optics Letters 9, 552 (1984)

[23] R.L.Fork, C.V.Shank, and R.Yin, Optecs Letters 8, 1 (1983)

[24] P.B.Allen, Phys.Rev.Lett.59, 1560 (1987)

[25] E.Heiner, phys.stat.sol.(b)148, 599 (1988)

[26] H.Elsayed-Ali, M.Pessot, T.Norris and G.Mourou, Phys.Rev.Lett.58, 1212 (1987)

[27] S.D.Brorson, W.Z.Lin, J.G.Fujimoto and E.P.Ippen, Phys.Rev.Lett. 59, 1962 (1987)

[28] R.H.M.Groeneveld, R.Sprik and A.Lagendijk, Phys.Rev.B64, 784 (1990)

[29] S.D.Brorson, A.Kazeroonian, J.S.Moodera, D.W.Face, T.K.Cheng, E.P.Ippen, M.S.Dresselhaus and G.Dresselhaus, Phys.Rev.Lett.64, 2172 (1990)

[30] O.Jepsen, D.Gloetzel, and A.R.Mackintosh, Phys.Rev.B23, 2684 (1981)
[31] A.H.MacDonald, J.M.Daams, S.H.Vosko, and D.D.Koelling, Phys.Rev.B (19 (198(1982)982)
[32] N.E.Christensen, phys.stat.sol.(b)54, 551 (1972)
[33] G.Lehmann and P.Ziesche, Elektronische Eigenschaften von Metallen, Akademie-Verlag, Berlin 1984
[34] M.Cardona, Modulation Spectroscopy, Academic Press, N.Y. 1969
[35] F.H.Pollak and O.J.Glembocki, Proc.SPIE 946,2 (1988)
[36] W.J.Scouler, Phys. Rev. Lett. 18, 445, (1967)
[37] R.Rosei and D.W.Lynch, Phys. Rev. B 5, 3883 (1972)
[38] C.A.Paddock and G.L.Eesley, J.Appl.Phys.60, 285 (1986)
[39] N.N.Bogoljubov, in: Studies in Statistical Mechanics I, J.de Boer and G.E.Uhlenbeck (eds.), North-Holland,
[40] N.N.Bogoljubov, Lectures on Quantum Statistics I, Gordon and Breach, N.Y. 1967
[41] A.R.Vasconcellos, A.C.Algarte and R.Luzzi, Physica A166, 517 (1990)
[42] J.M.Ziman, Electrons and Phonons, Oxford, London 1960
[43] D.L.Martin, Phys.Rev.170, 650 (1968)
[44] G.E.R.Schulze, Metallphysik, Akademie-Verlag, Berlin 1974
[45] W.Harrison, Electronic Structure and Properties of Solids, Part 2, Izd. Mir, Moskau 1983 (in Russian)
[46] U.Wenschuh and E.Heiner, phys.stat.sol(b)162, 303 (1990)
[47] H.Ehrenreich and M.H.Cohen,Phys.Rev.115,786(1959)
[48] W.Brauer und H.W.Streitwolf, Theor. Grdl. der Halbleiterphysik, Akademie-Verlag, Berlin, 1977. Amsterdam 1962
[49] J.Friedel, The Physics of Metals (J.M.Ziman, ed.), Cambridge University Press, New York, 1969
[50] R.Balian, Y.Allhassid, and H.Reinhardt, Phys. Rep. 131, 1 (1986)
[51] R.Kubo, Rep.Progr.Phys.29, 255 (1966)
[52] R.Kubo, J.Phys.Soc.Jpn.12, 570 (1957)
[53] E.Heiner, Physica A166, 633 (1990)

[54] Elk und W.Gasser, Die Methode der Greenschen Funktionen in der Festkörperphysik, Akademie-Verlag, Berlin 1978
[55] J.Lindhard, Kgl.Danske Videnskab. Selskab, Mat.-fys. Medd. 28, 8 (1954)
[56] F.Bloch, Phys.Rev.70, 460 (1946)
[57] Yu.A.Uspenski, E.G.Maksimov, S.N.Rashkeev, and I.I.Mazin, Z.Phys. B 53, 263 (1983)
[58] V.Fritzsche, phys.stat.sol(b)148, 395 (1988)
[59] W.Y.Liang and A.R.Beal, J.Phys.C9, 2823 (1976)
[60] U.Wenschuh and E.Heiner, phys.stat.sol(b)160, 225 (1990)
[61] M.Taut, in: P.Ziesche and G.Lehmann, Ergebnisse in der Elektronentheorie der Metalle, Akademie-Verlag, Berlin 1983, p.271, (1979)
[62] Landolt/Börnstein: Bd.I/4, Springer Verlag, Berlin, 1955, (p.82)
[63] American Institute of Physics Handbook; 3rd edition, McGraw Hill, New York, 1972
[64] E.Heiner, phys.stat.sol(b) 151, 645 (1989)
[65] F.Forstmann and R.R.Gerhardts, Metal Optics Near the Plasma Frequency, Springer Tracts in Modern Physics, Vol.109, Springer, Berlin 1986
[66] U.Wenschuh and E.Heiner, phys.stat.sol(b)163, K65 (1991)
[67] S.E.Schnatterly; Sol.Stat.Phys. 34, 275 (1979)
[68] P.B.Johnson and R.W.Christy, Phys.Rev.B6, 4370 (1972); Landolt/Börnstein Gruppe III, Band 15, Teilband b, Springer-Verlag, Berlin, Heidelberg 1983

Received by Publishing Department
on March 22, 1991.

Веншу У., Хайнер Э. E17-91-136

Об оптических свойствах ультрабыстрых переходов
в благородных металлах, возбужденных лазером

В случае, если электроны в металле могут быть непосредственно разогреты за промежуток времени меньший, чем время энергетической электрон-фононной релаксации, то возможно образование состояния с неравновесной температурой. Основываясь на системе дифференциальных уравнений, описывающей эволюцию электронной и фононной температуры в слоях благородных металлов, возбужденных лазерными импульсами ($\tau \approx 100$ фмс), а также на теории линейного отклика для систем, находящихся в состояниях, далеко от равновесия, проведена оценка зависящей от времени макроскопической диэлектрической функции (МДФ). Результаты модельных расчетов непосредственно измеряемой отражательной способности сравниваются с новым временным разрешением экспериментов.

Работа выполнена в Лаборатории теоретической физики ОИЯИ.
Сообщение Объединенного института ядерных исследований. Дубна 1991

Wenschuh U., Heiner E. E17-91-136

On the Theory of Ultrafast Transient Optical Properties
of Laser Excited Noble Metals

If the electrons in a metal can be directly heated on a time scale shorter than the electron-phonon energy relaxation time, a nonequilibrium temperature may be possible. Basing on a differential equation system describing the evolution of electron and phonon temperature in short puls ($\tau \approx 100$ fs) laser excited noble metal layers and a linear response theory for systems far from equilibrium a time dependent macroscopic dielectric function (MDF) is evaluated. The results of model calculations for the direct measurable reflectivity are compared with new time resolved experiments.

The investigation has been performed at the Laboratory of Theoretical Physics, JINR.

Communication of the Joint Institute for Nuclear Research. Dubna 1991